Industrial Chemistry & Materials

PAPER

Check for updates

Scalable copper-based coordination frameworks with tailored pore chemistry for energy-efficient C2H2/CO2 separation†

Hao-Ling Lan, Su-Tao Zheng, Li Xu, Guo-Wei Guan and Qing-Yuan Yang ![ORCID] *

The separation of C_2H_2/CO_2 mixtures for acetylene purification presents both industrial significance and fundamental challenges due to their nearly identical kinetic diameters and similar physical properties. This study demonstrates the effectiveness of ultramicroporous metal–organic frameworks (MOFs) in addressing this challenge through precise pore confinement effects. We introduce two ultramicroporous materials, Cu(cyhdc) and Cu(bdc), and assess their ability to capture C_2H_2. Under ambient conditions, Cu(cyhdc) and Cu(bdc) exhibit C_2H_2 uptakes of 1.92 mmol g^{-1} and 1.44 mmol g^{-1}, respectively. The most promising candidate is Cu(cyhdc), which possesses a C_2H_2/CO_2 selectivity of 8.45 at 298 K and 1 bar. Grand canonical Monte Carlo simulations revealed that the enhanced performance originates from multiple van der Waals interactions between C_2H_2 molecules and the curved cyclohexane-derived pore walls of Cu(cyhdc). Importantly, dynamic breakthrough experiments and scalable synthesis processes validated the practical separation potential of Cu(cyhdc) for C_2H_2/CO_2 mixtures. This work provides both mechanistic insights into gas–framework interactions and a potential solution for energy-efficient acetylene purification.

Keywords: C_2H_2/CO_2 separation; Ultramicroporous; Metal–organic framework; Pore confinement; Scalable synthesis.
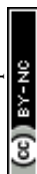
1 Introduction

The process of separating acetylene (C_2H_2) and carbon dioxide (CO_2) is a critical operation in various industrial applications, particularly in the field of acetylene purification.[1–5] Acetylene, a compound of carbon and hydrogen, is widely used in chemical synthesis and as a fuel in welding and cutting metals.[6–9] However, the presence of impurities such as CO_2 can significantly affect the quality and efficiency of these processes.[10–12] Therefore, it is essential to effectively separate C_2H_2 and CO_2. The challenge in this separation lies in the fact that acetylene and carbon dioxide share many similar physical properties and have nearly identical molecular sizes. This makes conventional separation techniques less effective, necessitating the development of more advanced and precise separation methods.[13–17] The complexity of this task has attracted significant scientific interest, leading to ongoing research and innovation in the field.

Metal–organic frameworks (MOFs) are widely recognized for their easily tunable pore sizes and geometries, as well as for their flexible internal surface modification.[18–21] By harnessing the isoreticular principle and a building-block strategy in MOF chemistry, researchers can now tailor the pore architecture of these materials with enhanced predictability and precision.[22–24] Through the strategic substitution of organic linkers and/or metal nodes, MOFs can be endowed with shape-matching capabilities and specific binding sites for targeted gas molecules.[25–27] In 2005, Matsuda, Kitaura and Kitagawa *et al.* first reported the use of a metal–organic framework (MOF) as a separating agent for the selective adsorption of acetylene (C_2H_2) over carbon dioxide (CO_2).[28] They selected a previously discovered copper-based MOF, $Cu_2(pzdc)_2(pyr)$, due to its distinctive structural features. The framework consists of two-dimensional Cu(pzdc) sheets interconnected with pyrazine pillars, forming one-dimensional channels with cross-sectional dimensions of 4 Å × 6 Å. These channels are fixed with basic adsorption sites, specifically oxygen atoms. By forming strong hydrogen bonds between the H atoms of C_2H_2 and O atoms of the MOF, C_2H_2 molecules are preferentially located in the middle of the channels. The saturation adsorbed amount of C_2H_2 at 298 K, 1 bar is 42 cm^3 g^{-1}. Another C_2H_2/CO_2 separation candidate is DICRO-4-Ni-i ([Ni(1,4-di(pyridine-2-yl)benzene)$_2$-(Cr_2O_7)]$_n$),[29]

State Key Laboratory of Fluorine & Nitrogen Chemicals, School of Chemical Engineering and Technology, Xi'an Jiaotong University, Xi'an, Shaanxi 710049, China. E-mail: qingyuan.yang@xjtu.edu.cn

which possesses an interpenetrated pcu topology consisting of $(Cr_2O_7)^{2-}$ pillars of the sql lattice built up from Ni^{2+} cations and di(pyridine-2-yl) benzene linkers. Benefitting from three types of channels with different pore chemistries, this new DICRO analogue has a higher C_2H_2 affinity with the framework and a C_2H_2 uptake twice the value of CO_2. The C_2H_2/CO_2 selectivity for an equimolar mixture was 13.9 at 1 bar, estimated using IAST. In the subsequent breakthrough test, a gas mixture consists of $C_2H_2/CO_2/He$ (10:5:85, v/v) at 1 bar, 298 K was studied. A slightly lower separation factor of 13 was calculated demonstrating the decent ability of this MOF for C_2H_2/CO_2 separation.[34,35] In recent years, an increasing number of high-performance MOFs for C_2H_2/CO_2 separation have been developed. Wang et al. reported two Cu-based MOFs, namely SIFSIX-dps-Cu and GeFSIX-dps-Cu, exhibiting high C_2H_2 uptake capacities of 4.57 mmol g^{-1} and 4.04 mmol g^{-1}, respectively. Notably, SIFSIX-dps-Cu achieved an impressive IAST selectivity of 1786.6 for equimolar (50/50) C_2H_2/CO_2.[13] Lin et al. reported UTSA-300a, which demonstrated exceptional IAST selectivity (>104) for equimolar C_2H_2/CO_2, enabling complete separation.[39] Additionally, Yang et al. developed CPL-1-NH₂, exhibiting a C_2H_2 uptake of 1.84 mmol g^{-1} and an IAST selectivity of 119 for equimolar C_2H_2/CO_2, rendering it a highly promising candidate for this separation.[40]

Herein, we demonstrate precise control over pore structures through altering the organic linkers in Cu(cyhdc) and Cu(bdc), thereby enhancing both C_2H_2 uptake capacity and C_2H_2/CO_2 selectivity. By incorporating different anionic linkers, two robust MOFs were synthesized with carefully modulated sub-nanometer pore cavities tailored for the demanding C_2H_2/CO_2 separation.[36–39] Optimization of pore dimensions combined with abundant binding sites retained the exclusive C_2H_2 adsorption behavior in Cu(cyhdc), resulting in a C_2H_2 uptake of 43.1 cm³ g^{-1} and a high IAST selectivity of 8.45. Molecular modeling and dynamic breakthrough experiments further confirmed the highly effective C_2H_2/CO_2 separation performance, particularly in Cu(cyhdc). Finally, we demonstrated the stable scale-up synthesis of Cu(cyhdc) and verified its phase purity.[30]

2 Results and discussion

The Cu(cyhdc) framework comprises one-dimensional chains of dicopper paddlewheel units interconnected with ditopic trans-1,4-cyclohexanedicarboxylate linkers, thereby forming a three-dimensional architecture characterized by rhombic channels oriented along the c axis.[31,32] Each copper center is coordinated with four equatorial carboxylate oxygen atoms, together with an axial carboxylate oxygen derived from an adjacent linker in the neighboring paddlewheel unit. In this context, flexible yet robust MOFs featuring permanently small pores and specific binding sites can be employed to selectively capture target gas molecules, while the co-adsorption of other gases is minimized by controlling the gate-opening pressure. This principle has been exemplified by Cu(cyhdc), which enables size-exclusive adsorption of C_2H_2 over CO_2. To achieve both high uptake capacity and superior separation selectivity for the more demanding C_2H_2/CO_2 separation, a systematic investigation into the fine-tuning of the pore structure in Cu(cyhdc) presents a rational approach (Fig. 1).

The powder X-ray diffraction (PXRD) patterns of Cu(cyhdc) and Cu(bdc) match well with the experimental PXRD data, confirming the phase purity of the bulk samples (Fig. 2a and b). Thermogravimetric analyses (TGA) were performed to evaluate the thermal stability of Cu(cyhdc). The TGA results suggest that Cu(cyhdc) is thermally stable before 300 °C (only 2.27% weight loss at 300 °C), suggesting its suitability for high-temperature conditions potentially encountered in industrial separation processes (Fig. S11†).

Nitrogen adsorption and desorption experiments were measured at 77 K to evaluate the permanent porosity. Cu(cyhdc) and Cu(bdc) both demonstrate typical type I adsorption isotherms, indicating their microporous nature. Surface areas from Brunauer–Emmett–Teller (BET) were assessed to be 490 m² g^{-1} for Cu(cyhdc) and 535 m² g^{-1} for Cu(bdc) based on the N₂ adsorption isotherm (Fig. S2†). Based on nonlocal density functional theory (NLDFT), Fig. S3† depicts the pore size distribution (PSD). The calculated PSD values for Cu(cyhdc) and Cu(bdc) are 0.76 nm and 0.58
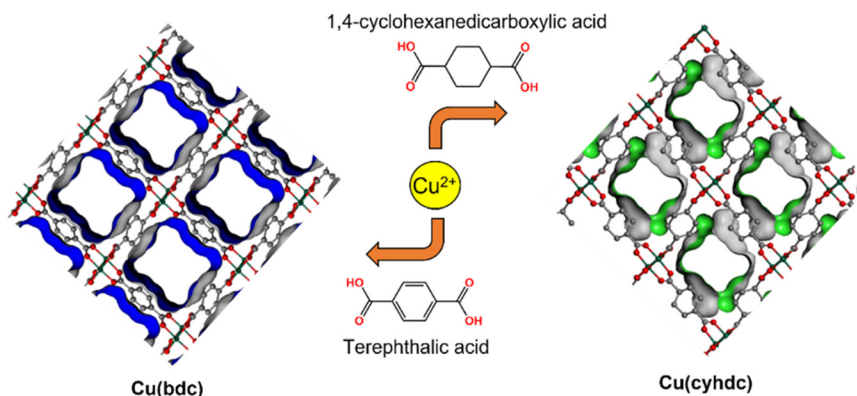

Fig. 1 Coordination configuration and pore structures of Cu(cyhdc) and Cu(bdc).
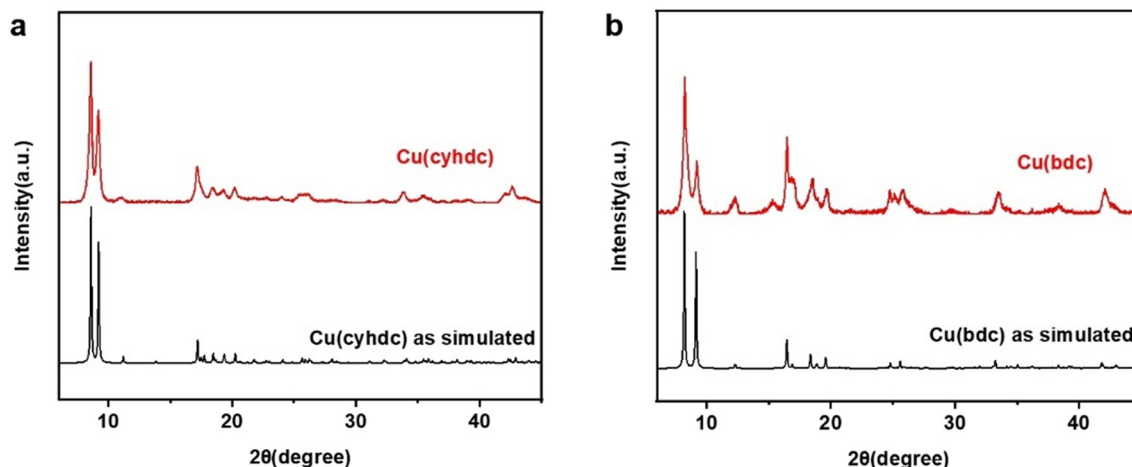
Fig. 2 PXRD patterns of (a) Cu(cyhdc) and (b) Cu(bdc).

nm, respectively. The smaller pore sizes of Cu(bdc) compared to those of Cu(cyhdc) are more likely attributed to the greater flexibility of the ligands *trans*-1,4-cyclohexanedicarboxylate in Cu(cyhdc), relative to 1,4-benzenedicarboxylate in Cu(bdc). According to the findings, different organic linkers might not only change the pore chemical environment but also modify the pore structure, leading to a higher affinity with C_2H_2 than CO_2 for both MOFs.

A series of gas adsorption experiments were conducted to evaluate the efficacy of Cu(cyhdc) and Cu(bdc) for the separation of C_2H_2 and CO_2. Single-component adsorption isotherms for C_2H_2 and CO_2 were measured at 273 K and 298 K. As depicted in Fig. 3a and b, Cu(cyhdc) exhibited C_2H_2 and CO_2 uptake capacities of 43.1 cm^3 g^{-1} and 22.7 cm^3 g^{-1}, respectively, at 298 K and 1 bar. In comparison, Cu(bdc) demonstrated uptake values of 32.4 cm^3 g^{-1} for C_2H_2 and 27.0 cm^3 g^{-1} for CO_2 under the same conditions. Notably, the C_2H_2 sorption amount of Cu(cyhdc) at 0.1 bar and 298 K was 23.0 cm^3 g^{-1}, which was far beyond that of Cu(bdc) (5.6 cm^3 g^{-1} at 0.1 bar and 298 K), indicating a greater affinity between C_2H_2 and Cu(cyhdc) frameworks. Despite the fact that Cu(bdc) has a smaller pore size of 5.8 Å compared to Cu(cyhdc) (7.6 Å), thus being more closely matched to the C_2H_2 diameter (3.4 Å), Cu(bdc) still adsorbs less C_2H_2 than Cu(cyhdc). The results showed stronger host–guest interactions between C_2H_2 and Cu(cyhdc) frameworks, likely due to the enhanced van der Waals interactions between the oxygen atoms in the Cu(cyhdc) framework and the hydrogen atoms of acetylene, compared to Cu(bdc). At 273 K and 1 bar, Cu(cyhdc) reached uptakes of 47.9 cm^3 g^{-1} for C_2H_2 and 44.9 cm^3 g^{-1} for CO_2 (Fig. 3c). Similarly, Cu(bdc) showed adsorption capacities of 49.7 cm^3 g^{-1} for C_2H_2 and 53.3 cm^3 g^{-1} for CO_2 at 273 K (Fig. 3d). These results underscore the potential of Cu(cyhdc) for C_2H_2/CO_2 separation under 1 bar and 298 K.

To elucidate the interaction strengths between C_2H_2/CO_2 and both MOFs, we determined the isosteric heat of adsorption (Q_{st}) by fitting adsorption isotherms to a virial

equation at 273 K and 298 K. For Cu(cyhdc), the zero-coverage Q_{st} values for C_2H_2 and CO_2 were found to be 36.6 and 22.1 kJ mol^{-1}, respectively (Fig. 4a). The substantial difference in adsorption enthalpy highlights the preferential adsorption of C_2H_2 over CO_2, thereby enhancing the separation efficacy of C_2H_2/CO_2 mixtures. In contrast, Cu(bdc) exhibited zero-coverage Q_{st} values of 24.4 and 21.0 kJ mol^{-1} for C_2H_2 and CO_2, respectively (Fig. 4a). These findings indicate that Cu(cyhdc) possesses a stronger affinity for C_2H_2, emphasizing its potential as an effective material for the selective separation of C_2H_2/CO_2 gas mixtures. Motivated by these observations, we evaluated the adsorption selectivities of a C_2H_2/CO_2 binary mixture using ideal adsorbed solution theory (IAST) at 298 K. The calculated IAST selectivities for C_2H_2/CO_2 (5 : 5) in Cu(cyhdc) and Cu(bdc) were 8.45 and 1.65, respectively, at 100 kPa (Fig. 4b). The enhanced selectivity of Cu(cyhdc) is attributable to its stronger affinity for C_2H_2 molecules. Notably, the selectivity of C_2H_2/CO_2 (5 : 5) in Cu(cyhdc) surpasses that of several benchmark metal–organic frameworks (MOFs) employed for C_2H_2/CO_2 separation, including SIFSIX-3-Ni,[32] TIFSIX-2-Cu-I,[33] JNU-1,[34] UTSA-222a,[35] and FJU-90a (Fig. 4c).[35] Combined with its decent adsorption capacity, Cu(cyhdc) effectively mitigates the conventional trade-off between capacity and selectivity. Consequently, Cu(cyhdc) emerges as a highly efficient material for the separation of C_2H_2/CO_2 mixtures.

Grand canonical Monte Carlo (GCMC) and density functional theory (DFT) calculations were performed to elucidate the adsorption interactions between C_2H_2 and CO_2 molecules and their respective binding sites. For Cu(cyhdc), as illustrated in Fig. 5, the hydrogen atoms of C_2H_2 engage with the framework through O–H···π electrostatic contacts (ranging from 2.92 to 3.28 Å) and induced-dipole interactions between its saturated carbon backbone and the C_2H_2 molecules. In contrast, CO_2 exhibited significantly longer binding distances to the framework, spanning 3.71 to 4.30 Å. These computational results are consistent with the experimentally determined Q_{st} values for C_2H_2 and CO_2 (36.6

© 2025 The Author(s). Co-published by the Institute of Process Engineering, Chinese Academy of Sciences and the Royal Society of Chemistry
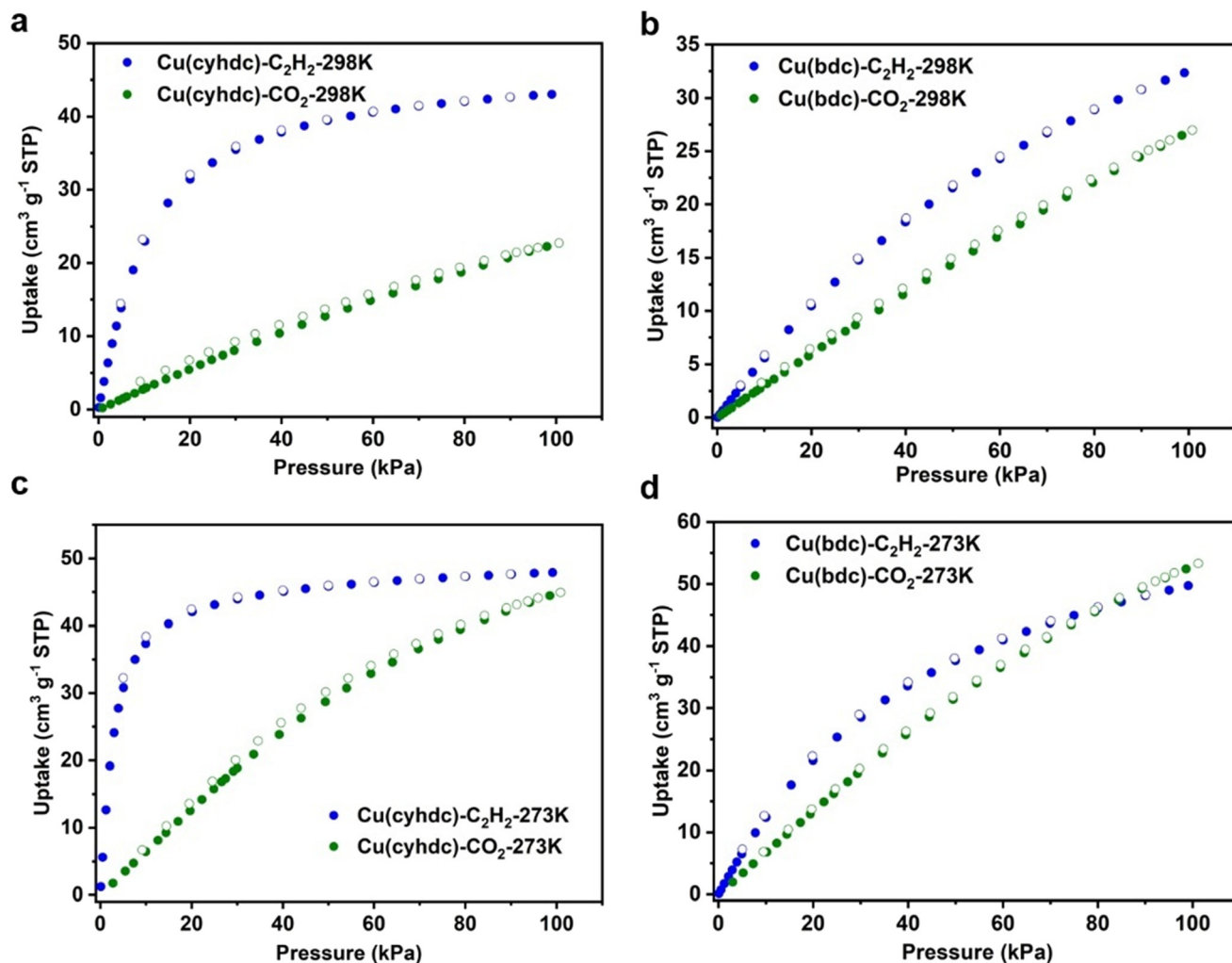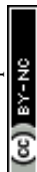
Ind. Chem. Mater., 2025, **3**, 723–731 | **725**

Fig. 3 C_2H_2 and CO_2 adsorption isotherms of (a) Cu(cyhdc) and (b) Cu(bdc) at 298 K; (c) Cu(cyhdc) and (d) Cu(bdc) at 273 K.

and 22.1 kJ mol^{-1}, respectively), thereby reaffirming the preferential adsorption of C_2H_2 over CO_2 in Cu(cyhdc). For Cu(bdc), as shown in Fig. 5, the binding distances of C_2H_2 to the framework were slightly longer (3.24–3.37 Å) compared to those in Cu(cyhdc), which accounts for the lower C_2H_2 adsorption capacity observed in Cu(bdc) (32.3 cm^3 g^{-1}) relative to Cu(cyhdc) (43 cm^3 g^{-1}). The variation in bond lengths confirms that the organic linker *trans*-1,4-cyclohexanedicarboxylate exhibits a stronger affinity for C_2H_2 than 1,4-benzenedicarboxylate, thereby making Cu(cyhdc) a superior candidate for C_2H_2/CO_2 separation.

Although the pore size of Cu(bdc) (5.8 Å) is more compatible with the size of acetylene molecules compared to that of Cu(cyhdc) (7.6 Å), experimental data indicate that Cu(cyhdc) exhibits a higher acetylene adsorption capacity than Cu(bdc). To further explore the interaction mechanisms between acetylene molecules and the two frameworks with the same metal center, the influence of the organic ligands is a key factor. Firstly, the saturated six-membered ring structure of the cyclohexane ligand (cyhdc) adopts a chair conformation, which may lead to the formation of more

complex channel structures within the MOF framework. This flexibility allows the channels to dynamically adjust during adsorption, better matching the size of acetylene molecules (linear structure and a kinetic diameter of approximately 3.3 Å), thus enhancing the adsorption capacity. In contrast, the planar rigid structure of the terephthalic acid (bdc) ligand may result in fixed pore sizes in Cu(bdc), leading to a poorer fit for acetylene. Secondly, the saturated carbon backbone of cyclohexane may induce stronger van der Waals interactions with acetylene's π-electron cloud through dipole-induced interactions. The conjugated π-system of the benzene ring, however, could form competitive repulsive interactions with the acetylene π-bond, reducing the adsorption efficiency. Finally, the flexible framework of Cu(cyhdc) may undergo local structural relaxation during acetylene adsorption, expanding the channels or optimizing the arrangement of adsorption sites, thus increasing the adsorption capacity. On the other hand, the rigid framework of Cu(bdc) may not achieve similar dynamic adjustments.

To assess the separation efficacy of Cu(cyhdc) for C_2H_2/CO_2 mixtures, dynamic breakthrough experiments were

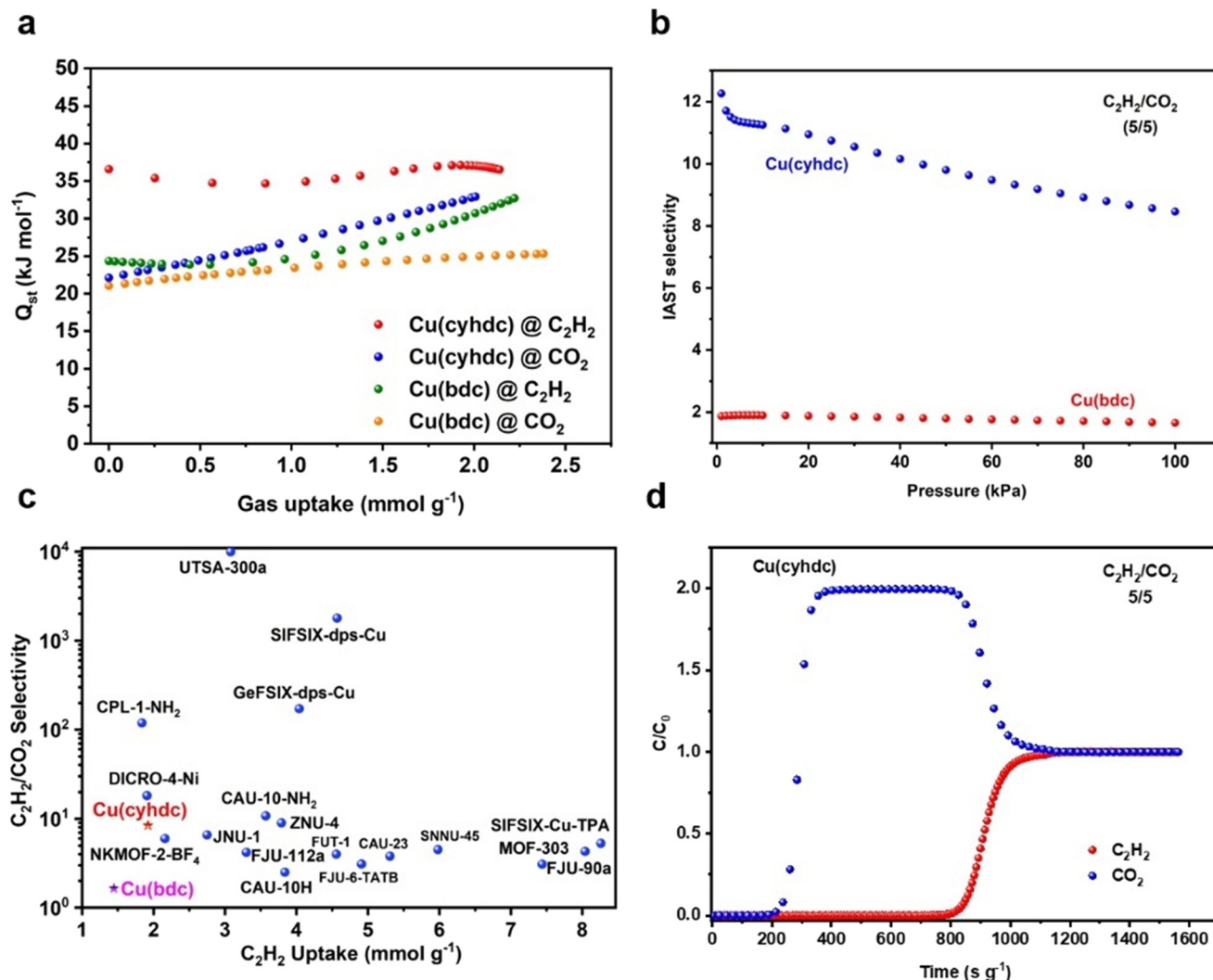Fig. 4 (a) Isosteric heats of adsorption (Q_{st}) of C_2H_2 and CO_2 in Cu(cyhdc) and Cu(bdc); (b) IAST selectivity of C_2H_2/CO_2 for Cu(cyhdc) and Cu(bdc); (c) C_2H_2 uptakes and C_2H_2/CO_2 selectivity comparison with some benchmark materials at 298 K and 100 kPa; (d) experimental breakthrough curves of C_2H_2/CO_2 (5/5) for Cu(cyhdc) at 298 K and 1 bar.

conducted at 298 K and 1 bar using laboratory-scale equipments. A binary C_2H_2/CO_2 gas mixture (5/5) was passed through a packed column containing activated Cu(cyhdc) samples. The outlet gas concentrations were monitored with an INFICON mass spectrometer. As illustrated in Fig. 4d, CO_2 exhibited a breakthrough at 332.9 s g^{-1} and rapidly reached a plateau, whereas the C_2H_2 breakthrough was significantly delayed, occurring at 1203.7 s g^{-1}. These results demonstrate that Cu(cyhdc) effectively separates C_2H_2 from CO_2 under ambient conditions.

Finally, we investigated the scale-up synthesis of Cu(cyhdc) by maintaining the reaction conditions and post-synthesis procedures unchanged, while increasing the quantities of reactants tenfold and solvents eightfold. The reactants and solvents were added in a 1 L bottle with continuous stirring. Following approximately 20 minutes of ultrasonic dissolution, a clear blue solution was obtained

and it was placed in an oven for reaction. As shown in Fig. S8,† we carried out 5 batches of kilogram-scale synthesis of Cu(cyhdc), with yields of 79.1%, 75.5%, 81.9%, 76.6% and 76.4%, respectively. Unlike the previously reported synthesis procedure (yielded about 2 g per batch), this method yielded approximately 1550 g of bulk Cu(cyhdc) with a total yield of 77.9%. Powder X-ray diffraction (PXRD) analysis of the bulk samples was consistent with that of laboratory-scale products (Fig. 6), confirming the phase purity of the scaled-up material. Cu(cyhdc) satisfies key green chemistry criteria through cost-effective copper precursors (~18 CNY per kg), energy-efficient synthesis (90 °C/18 h without pressurized equipment), and exceptional stability (300 °C thermal tolerance; 60% RH/6 month durability). These advantages, combined with the future potential for DMF solvent recycling to reduce production costs, position it as a sustainable material for industrial implementation.[30]
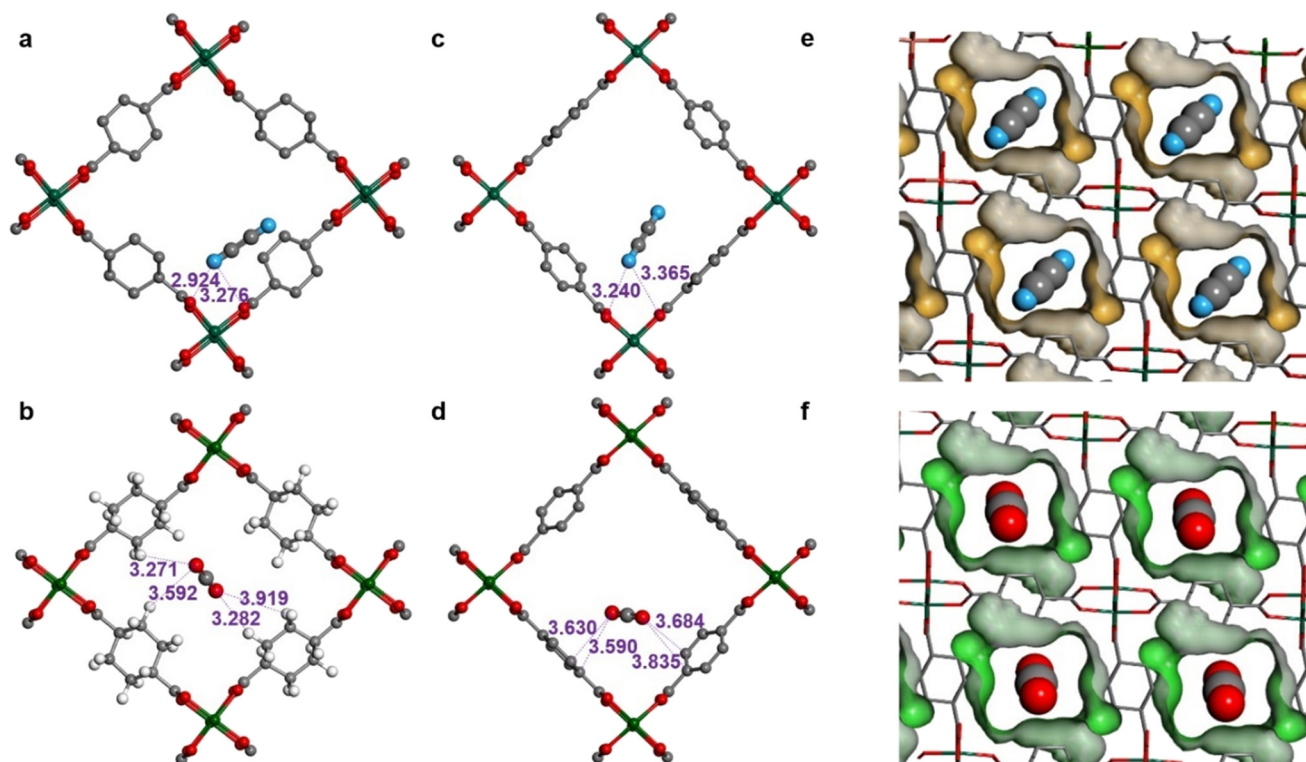
© 2025 The Author(s). Co-published by the Institute of Process Engineering, Chinese Academy of Sciences and the Royal Society of Chemistry

Ind. Chem. Mater., 2025, **3**, 723–731 | **727**

Fig. 5 Preferential binding sites of (a) C_2H_2 and (b) CO_2 in Cu(cyhdc) determined by GCMC simulations; preferential binding sites of (c) C_2H_2 and (d) CO_2 in Cu(bdc) determined by GCMC simulations; the unit of distance is Å. Cu, dark green; O, red; C, grey; H, pale grey. H atoms of (a), (c) and (d) are omitted for clarity. GCMC simulations of guest-inclusion structures for (e) C_2H_2 loaded Cu(cyhdc) and (f) CO_2 loaded Cu(cyhdc).
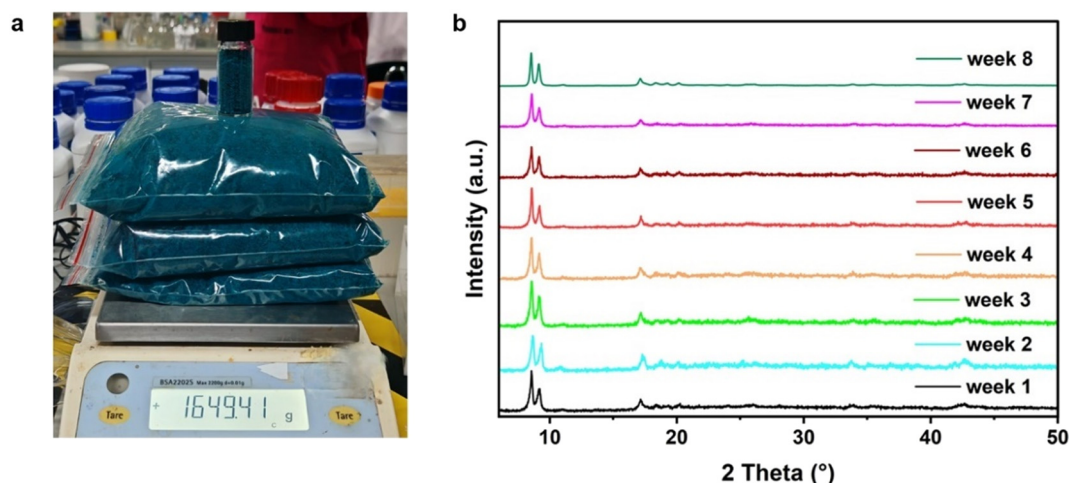

Fig. 6 (a) Products of kilogram-scale synthesis of Cu(cyhdc); (b) PXRD patterns of kilogram-scale Cu(cyhdc) recorded over an 8-week ageing test (50 °C, 60% RH; samples taken weekly).

3 Conclusions

This study presents two copper-based coordination frameworks for the separation of C_2H_2/CO_2 mixtures. Compared to other porous materials, Cu(cyhdc) exhibits a well-balanced C_2H_2 adsorption capacity and C_2H_2/CO_2 selectivity. Owing to its flexible organic ligand, *trans*-1,4-cyclohexanedicarboxylate, Cu(cyhdc) demonstrates a stronger affinity for C_2H_2 molecules, resulting in enhanced C_2H_2/CO_2 selectivity. Theoretical calculations were conducted to elucidate the underlying mechanisms of C_2H_2 adsorption and separation, revealing that C_2H_2 interacts more strongly with the framework than CO_2. Column breakthrough experiments further confirmed that Cu(cyhdc) efficiently separates C_2H_2/CO_2 mixtures. Additionally, our laboratory has successfully achieved a scalable synthesis of Cu(cyhdc) at

the 10 kg scale, while maintaining a cost control of approximately 200 RMB per kilogram. The scalable synthesis method of Cu(cyhdc) positions it as a promising adsorbent for future applications, offering high efficiency and low energy consumption in C_2H_2 capture and separation.

4 Experimental section

4.1 Materials

trans-1,4-Cyclohexanedicarboxylic acid (97%) and *N,N*-dimethylformamide (DMF, ≥99%) were purchased from Aladdin Bio-Chem Technology Co. Ltd. Terephthalic acid (99%) and copper(II) nitrate trihydrate (AR, 99%) were purchased from Shanghai Macklin Biochemical Technology Co. Ltd.

4.2 Synthesis of Cu(cyhdc)

Cu(cyhdc) was prepared according to a previously reported method with a slight modification.[33] For Cu(cyhdc), *trans*-1,4-cyclohexanedicarboxylic acid (1.722 g, 0.01 mol) and $Cu(NO_3)_2 \cdot 3H_2O$ (2.416 g, 0.01 mol) were added to a 250 mL bottle charged with 100 mL *N,N*-dimethylformamide. After about 2 minutes of ultrasonic dissolution, the blue solution was heated for 16 h in an oven at 90 °C. The obtained precipitate, exhibiting a green-blue hue, was isolated through filtration and subsequently washed thrice using 25 mL portions of fresh *N,N*-dimethylformamide. This step was followed by another series of washes, where the precipitate was rinsed thrice with 25 mL portions of methanol, then immersed in 100 mL fresh methanol for 24 h (two times) and then preserved in 100 mL of fresh methanol within a tightly sealed bottle. The framework was activated by heating at 150 °C under vacuum for 18 h to 24 h and a deep green powder was obtained.

4.3 Synthesis of Cu(bdc)

The framework Cu(bdc) was prepared using a modification of the procedure reported in ref. 33. The procedure is almost identical to that of Cu(cyhdc), except that a different organic ligand is used. For Cu(bdc), terephthalic acid (1.661 g, 0.01 mol) and $Cu(NO_3)_2 \cdot 3H_2O$ (2.416 g, 0.01 mol) were added to a 250 mL bottle charged with 100 mL *N,N*-dimethylformamide. After stirring and dissolving, the blue solution was heated for 16 h in an oven at 90 °C. The obtained precipitate, exhibiting a blue hue, was isolated through filtration and subsequently washed thrice using 25 mL portions of fresh *N,N*-dimethylformamide. This step was followed by another series of washes, where the precipitate was rinsed thrice with 25 mL portions of methanol, then immersed in 100 mL fresh methanol for 24 h (two times) and then preserved in 100 mL of fresh methanol within a tightly sealed bottle. The framework was activated by heating at 150 °C under vacuum for 18 h to 24 h and a darker blue powder was obtained.

4.4 Characterization

The phase purities of Cu(cyhdc) and Cu(bdc) were determined by powder X-ray diffraction (PXRD). A LabXXRD-6100: SHIMADZU (Shimadzu Corporation, Kyoto, Japan) with a CuK radiation source (λ = 1.5406 Å) was used to collect the diffractograms from 5 to 60° (2θ). To determine the thermogravimetric (TGA) curves, a Netzsch STA449F5 instrument was used in a nitrogen atmosphere (nitrogen flow rate of 100 mL min^{-1}). In closed alumina cells, the sample was heated at 20 °C min^{-1} between 25 and 300 °C to perform this experiment. To study the surface morphology of the two MOFs, a TESCAN MAIA3 LMH scanning electron microscope was used.

4.5 Gas adsorption measurements

BSD-PM2 (Beishide Instrument Technology (Beijing) Co. Ltd.) and JW-BK200C (JWGB Sci & Tech Co. Ltd.) instruments were used to measure C_2H_2, CO_2, and N_2 adsorption isotherms at various temperatures (273–298 K). Prior to gas adsorption measurements, both MOFs were evacuated at 150 °C for 24 h. During sorption experiments, the temperatures were precisely controlled with anhydrous ethanol in a constant temperature bath. The cryogenic temperatures were maintained using liquid nitrogen baths at 77 K.

4.6 Breakthrough separation experiments

With dynamic breakthrough equipment (BSD-MAB, Beishide Instrument Technology (Beijing) Co. Ltd.), dynamic breakthrough experiments were carried out at 101 kPa and 298 K. For this, C_2H_2/CO_2 gas mixtures (50/50, v/v) were used. A glass column filled with 0.7 g of activated Cu(cyhdc) was used for the experiments. The column has a diameter of 6 mm and a length of 20 cm. The length of the packed MOF sample was 6.7 cm. Prior to breakthrough experiments, the columns were degassed for 10 h at 150 °C under vacuum. After degassing, the columns were swept with 40 mL min^{-1} of He at room temperature. Using a gas flow meter, the total C_2H_2/CO_2 gas flow rate at the entrance was set to 4 mL min^{-1}. The gases emitted from the adsorption bed were continuously monitored using a BSD mass spectrometer (thermal conductivity detector (TCD), 1 ppm detection limit).

Data availability

Additional supporting data, such as XRD patterns, adsorption isotherms, and TEM images, are included in the ESI† of this paper. Specific datasets related to the molding of porous materials are subject to confidentiality agreements but may be accessed for academic purposes upon reasonable request to the corresponding author (email: qingyuan.yang@xjtu.edu.cn).

Conflicts of interest

The authors declare no conflict of interest.

© 2025 The Author(s). Co-published by the Institute of Process Engineering, Chinese Academy of Sciences and the Royal Society of Chemistry

Ind. Chem. Mater., 2025, **3**, 723–731 | 729

Acknowledgements

References

1 H. Schobert, Production of acetylene and acetylene-based chemicals from coal, *Chem. Rev.*, 2014, **114**, 1743–1760.

2 K. Chen, D. G. Madden, S. Mukherjee, T. Pham, K. A. Forrest, A. Kumar, B. Space, J. Kong, Q. Zhang and M. J. Zaworotko, Synergistic sorbent separation for one-step ethylene purification from a four-component mixture, *Science*, 2019, **366**, 241–246.

3 X. Huang, D. Cheng, F. Chen and X. Zhan, The decomposition of aromatic hydrocarbons during coal pyrolysis in hydrogen plasma: A density functional theory study, *Int. J. Hydrogen Energy*, 2012, **37**, 18040–18049.

4 Y. He, F. Chen, B. Li, G. Qian, W. Zhou and B. Chen, Porous metal-organic frameworks for fuel storage, *Coord. Chem. Rev.*, 2018, **373**, 167–198.

5 H. Wang, W. P. Lustig and J. Li, Sensing and capture of toxic and hazardous gases and vapors by metal-organic frameworks, *Chem. Soc. Rev.*, 2018, **47**, 4729–4756.

6 E. Bartholomé, The BASF-process for production of acetylene by partial oxidation of gaseous hydrocarbons, *Chem. Eng. Sci.*, 1954, **3**, 94–104.

7 T. Ren, M. K. Patel and K. Blok, Steam cracking and methane to olefins: Energy use, CO_2 emissions and production costs, *Energy*, 2008, **33**, 817–833.

8 Q. Zhang, Y. Liu, T. Chen, X. Yu, J. Wang and T. Wang, Simulations of methane partial oxidation by CFD coupled with detailed chemistry at industrial operating conditions, *Chem. Eng. Sci.*, 2016, **142**, 126–136.

9 L. Yang, S. Qian, X. Wang, X. Cui, B. Chen and H. Xing, Energy-efficient separation alternatives: Metal-organic frameworks and membranes for hydrocarbon separation, *Chem. Soc. Rev.*, 2020, **49**, 5359–5406.

10 J. Li, L. Jiang, S. Chen, A. Kirchon, B. Li, Y. Li and H. Zhou, Metal–organic framework containing planar metal-binding sites: Efficiently and cost-effectively enhancing the kinetic separation of C_2H_2/C_2H_4, *J. Am. Chem. Soc.*, 2019, **141**, 3807–3811.

11 X. Cui, K. Chen, H. Xing, Q. Yang, R. Krishna, Z. Bao, H. Wu, W. Zhou, X. Dong, Y. Han, B. Li, Q. Ren, M. J. Zaworotko and B. Chen, Pore chemistry and size control in hybrid porous materials for acetylene capture from ethylene, *Science*, 2016, **353**, 141–144.

12 Y. Du, Y. Chen, Y. Wang, C. He, J. Yang, L. Li and J. Li, Optimized pore environment for efficient high selective C_2H_2/C_2H_4 and C_2H_2/CO_2 separation in a metal-organic framework, *Sep. Purif. Technol.*, 2021, **256**, 117749.

13 J. Wang, Y. Zhang, Y. Su, X. Liu, P. Zhang, R. Lin, S. Chen, Q. Deng, Z. Zeng, S. Deng and B. Chen, Fine pore engineering in a series of isoreticular metal-organic frameworks for efficient C_2H_2/CO_2 separation, *Nat. Commun.*, 2022, **13**, 200.

14 S. Wang, H. Lan, G. Guan and Q. Yang, Amino functionalized microporous MOFs for capturing greenhouse gases CF_4 and NF_3 with record selectivity, *ACS Appl. Mater. Interfaces*, 2022, **14**, 40072–40081.

15 J. Lin, T. T. T. Nguyen, R. Vaidhyanathan, J. Burner, J. M. Taylor, H. Durekova, F. Akhtar, R. K. Mah, O. Ghaffari-Nik, S. Marx, N. Fylstra, S. S. Iremonger, K. W. Dawson, P. Sarkar, P. Hovington, A. Rajendran, T. K. Woo and G. K. H. Shimizu, A scalable metal-organic framework as a durable physisorbent for carbon dioxide capture, *Science*, 2021, **374**, 1464–1469.

16 W. Fan, S. B. Peh, Z. Zhang, H. Yuan, Z. Yang, Y. Wang, K. Chai, D. Sun and D. Zhao, Tetrazole-functionalized zirconium metal-organic cages for efficient C_2H_2/C_2H_4 and C_2H_2/CO_2 separations, *Angew. Chem., Ind. Ed.*, 2021, **60**, 17338–17343.

17 F. Illuzzi and H. Thewissen, Perfluorocompounds emission reduction by the semiconductor Industry, *J. Integr. Environ. Sci.*, 2010, **7**, 201–210.

18 C. Li, H. Zhang, M. Liu, F. Lang, J. Pang and X. Bu, Recent progress in metal-organic frameworks (MOFs) for electrocatalysis, *Ind. Chem. Mater.*, 2023, **1**, 9–38.

19 S. Wang, X. Mu, H. Liu, S. Zheng and Q. Yang, Pore-structure control in metal-organic frameworks (MOFs) for capture of the greenhouse gas SF_6 with record separation, *Angew. Chem.*, 2022, **61**, e202207066.

20 X. Zhan, R. Wang, J. Zhang and X. Chen, Plastic pores for switchable and optimized adsorption behaviors, *ACS Cent. Sci.*, 2025, **11**, 479–485.

21 K. Adil, Y. Belmabkhout, R. S. Pillai, A. Cadiau, P. M. Bhatt, A. H. Assen, G. Maurin and M. Eddaoudi, Gas/vapour separation using ultra-microporous metal-organic frameworks: Insights into the structure/separation relationship, *Chem. Soc. Rev.*, 2017, **46**, 3402.

22 T. Wang, M. Chang, T. Yan, Y. Ying, Q. Yang and D. Liu, Calcium-based metal−organic framework for efficient capture of sulfur hexafluoride at low concentrations, *Ind. Eng. Chem. Res.*, 2021, **60**, 5976–5983.

23 S. Wang, M. Shivanna and Q. Yang, Nickel-based metal−organic frameworks for coal-bed methane purification with Record CH_4/N_2 selectivity, *Angew. Chem.*, 2022, **134**, e202201017.

24 S. Wang and Q. Yang, A copper-based metal-organic framework for upgrading natural gas through the recovery of C_2H_6 and C_3H_8, *Green Chem. Eng.*, 2022, **4**, 81–87.

25 J. Zou, Z. Wang, Y. H. Andaloussi, J. Xue, W. Zhang, B. E. G. Lucier, M. J. Zaworotko, G. Chen, S. Chen and Y. Peng, Benchmarking selective capture of trace CO_2 from C_2H_2 using an amine-functionalized adsorbent, *Nat. Commun.*, 2025, **16**, 2598.

26 J. Pang, F. Jiang, M. Wu, C. Liu, K. Su, W. Lu, D. Yuan and M. Hong, A porous metal-organic framework with ultrahigh acetylene uptake capacity under ambient conditions, *Nat. Commun.*, 2015, **6**, 7575.

27 D. Li and K. Kaneko, Molecular geometry-sensitive filling in semi-rectangular mircopores of organic-inorganic hybrid crystals, *J. Phys. Chem. B*, 2000, **104**, 8940–8945.

28 R. Matsuda, R. Kitaura, S. Kitagawa, Y. Kubota, R. V. Belosludov, T. C. Kobayashi, H. Sakamoto, T. Chiba, M. Takata, Y. Kawazoe and Y. Mita, Highly controlled acetylene accommodation in a metal–organic microporous material, *Nature*, 2005, **436**, 238–241.

29 H. S. Scott, M. Shivanna, A. Bajpai, D. G. Madden, K. Chen, T. Pham, K. A. Forrest, A. Hogan, B. Space, J. J. Perry Iv and M. J. Zaworotko, Highly selective separation of C_2H_2 from CO_2 by a new dichromate-based hybrid ultramicroporous material, *ACS Appl. Mater. Interfaces*, 2017, **9**, 33395–33400.

30 P. A. Julien, C. Mottillo and T. Friscic, Metal-organic frameworks meet scalable and sustainable synthesis, *Green Chem.*, 2017, **19**, 2729–2747.

31 H. Kumagai, M. Akita-Tanaka, K. Inoue, K. Takahashi, H. Kobayashi, S. Vilminot and M. Kurmoo, Metal-organic frameworks from copper dimers with cis- and trans- 1,4-cyclohexanedicarboxylate and cis, cis- 1,3,5-cyclohexanetricarboxylate, *Inorg. Chem.*, 2007, **46**, 5949–5956.

32 C. G. Carson, G. Brunnello, S. Geol Lee, S. Soon Jang, R. A. Gerhardt and R. Tannenbaum, Structure solution from powder diffraction of copper 1,4- benzenedicarboxylate, *Eur. J. Inorg. Chem.*, 2014, **12**, 2140–2145.

33 B. E. R. Snyder, A. B. Turkiewicz, H. Furukawa, M. V. Paley, E. O. Velasquez, M. N. Dods and J. R. Long, A ligand insertion mechanism for cooperative NH_3 capture in metal–organic frameworks, *Nature*, 2023, **613**, 287–291.

34 K. Chen, H. S. Scott, D. G. Madden, T. Pham and M. J. Zaworotko, Benchmark C_2H_2/CO_2 and CO_2/C_2H_2 separation by two closely related hybrid ultramicroporous materials, *Chem*, 2016, **1**, 753–765.

35 H. Zeng, X. Mo, Y. Huang, Y. Zhao, X. Xie and D. Li, Induced fit of C_2H_2 in a flexible MOF through cooperative action of open metal sites, *Angew. Chem., Int. Ed.*, 2019, **58**, 8515–8519.

36 J. Ma, J. Guo, H. Wang, B. Li, T. Yang and B. Chen, Microporous lanthanide metal-organic framework constructed from lanthanide metalloligand for selective separation of C_2H_2/CO_2 and C_2H_2/CH_4 at room temperature, *Inorg. Chem.*, 2017, **56**, 7145–7150.

37 Y. Ye, Z. Ma, R. Lin, R. Krishna, W. Zhou, Q. Lin, Z. Zhang, S. Xiang and B. Chen, Pore space partition within a metal-organic framework for highly efficient C_2H_2/CO_2 separation, *J. Am. Chem. Soc.*, 2019, **141**, 4130–4136.

38 Q. Zhu, Y. Zeng and Y. Zheng, Overview of CO_2 capture and electrolysis technology in molten salts: Operational parameters and their effects, *Ind. Chem. Mater.*, 2023, **1**, 595–617.

39 R. Lin, L. Li, H. Wu, H. Arman, R. Bin Li, W. Lin and B. Chen Zhou, Optimized separation of acetylene from carbon dioxide and ethylene in a microporous material, *J. Am. Chem. Soc.*, 2017, **139**, 8022–8028.

40 L. Yang, L. Yan, Y. Wang, Z. Liu, J. He, Q. Fu, D. Liu, X. Gu, P. Dai, L. Li and X. Zhao, Adsorption site selective occupation strategy within a metal-organic framework for highly efficient sieving acetylene from carbon dioxide, *Angew. Chem., Int. Ed.*, 2021, **60**, 4570–4574.

© 2025 The Author(s). Co-published by the Institute of Process Engineering, Chinese Academy of Sciences and the Royal Society of Chemistry

Ind. Chem. Mater., 2025, **3**, 723–731 | **731**